New BIOTECHNOLOGY 78 (2023) 1–12

Contents lists available at ScienceDirect

New BIOTECHNOLOGY

journal homepage: www.elsevier.com/locate/nbt

Transcription factor-based biosensors for detection of naturally occurring phenolic acids

Ernesta Augustiniene [a], Ingrida Kutraite [a], Egle Valanciene [a], Paulius Matulis [a], Ilona Jonuskiene [a], Naglis Malys [a,b,*]

[a] Bioprocess Research Centre, Faculty of Chemical Technology, Kaunas University of Technology, Radvilenu st. 19, LT-50254 Kaunas, Lithuania
[b] Department of Organic Chemistry, Faculty of Chemical Technology, Kaunas University of Technology, Radvilenu st. 19, LT-50254 Kaunas, Lithuania

ARTICLE INFO

Keywords:
Whole-cell biosensor
Transcription factor
Inducible gene expression system
Phenolic acid

ABSTRACT

Phenolic acids including hydroxybenzoic and hydroxycinnamic acids are secondary plant and fungal metabolites involved in many physiological processes offering health and dietary benefits. They are often utilised as precursors for production of value-added compounds. The limited availability of synthetic biology tools, such as whole-cell biosensors suitable for monitoring the dynamics of phenolic acids intracellularly and extracellularly, hinders the capabilities to develop high-throughput screens to study their metabolism and forward engineering. Here, by applying a multi-genome approach, we have identified phenolic acid-inducible gene expression systems composed of transcription factor-inducible promoter pairs responding to eleven different phenolic acids. Subsequently, they were used for the development of whole-cell biosensors based on model bacterial hosts, such as *Escherichia coli*, *Cupriavidus necator* and *Pseudomonas putida*. The dynamics and range of the biosensors were evaluated by establishing their response and sensitivity landscapes. The specificity and previously uncharacterised interactions between transcription factor and its effector(s) were identified by a screen of twenty major phenolic acids. To exemplify applicability, we utilise a protocatechuic acid-biosensor to identify enzymes with enhanced activity for conversion of *p*-hydroxybenzoate to protocatechuate. Transcription factor-based biosensors developed in this study will advance the analytics of phenolic acids and expedite research into their metabolism.

Introduction

Phenolic acids including hydroxybenzoic and hydroxycinnamic acids are important antioxidants and antimicrobial agents utilised in various industries, including food, pharmaceutical, cosmetics, and chemical [1]. They are mainly extracted from plants, but recently, the use of microbial cell factories based on *Escherichia coli, Streptomyces* sp., *Corynebacterium glutamicum, Pseudomonas* sp., *Bacillus* sp., *Amycolatopsis* sp., and *Klebsiella pneumonia* has come into focus as a sustainable alternative for their production [2]. In this effort, the forward engineering and screening of producing strains often relies on chromatography-based techniques such as high-performance liquid chromatography (HPLC) coupled with a photodiode array detector or some other more rarely utilised physicochemical methods [3]. They require complex sample preparation including extraction, filtration, and often chemical treatment. Despite such analysis methods being robust and delivering highly reproducible data, they are usually labour-intensive, expensive and of low throughput.

Recently, inducible gene expression systems, composed of chemical molecule-responsive transcription factor (TF) and cognate inducible promoter, have come into the focus as a platform for genetically encoded TF-based whole-cell biosensors that can be used as an *in vivo* analytical tool for extracellular and intracellular metabolite analysis. The interaction of TFs with specific effectors, or so-called ligand molecules, activates the expression of the reporter protein in a dose dependent manner, resulting in quantitatively measurable output [4]. TF-based biosensors have been employed in synthetic biology, enabling high-throughput strategies for strain screening and development [5].

Abbreviations: HPLC, high-performance liquid chromatography; TF, transcription factor; ANF, absolute normalised fluorescence values; RFP, red fluorescent protein; PDC, phenolic acid decarboxylase; PobA, 4-hydroxybenzoate 3-monooxygenase; Fcs, feruloyl-CoA synthetase; TCA, tricarboxylic acid; hca, hydroxycinnamate.

* Corresponding author at: Bioprocess Research Centre, Faculty of Chemical Technology, Kaunas University of Technology, Radvilenu st. 19, LT-50254 Kaunas, Lithuania.

E-mail address: naglis.malys@ktu.lt (N. Malys).

https://doi.org/10.1016/j.nbt.2023.09.004
Received 9 January 2023; Received in revised form 9 June 2023; Accepted 12 September 2023
Available online 14 September 2023

They have played an important role in the development of technologies for detection of target molecules at the single-cell level [4], screening of producer strains [6] or enzymes [7], monitoring the degradation of biopolymers [8] and valorisation of lignocellulose [9]. To expand their application range, research has been directed towards altering biosensor specificity through TF engineering [9,10], optimisation of biosensor-based high-throughput screening [11], and other improvements [9,12–15].

In this study, the focus is on the development of TF-based biosensors for the detection of phenolic acids. Systematically, phenolic acid-responsive-inducible gene expression systems and their key genetic elements were identified by applying a multi-genome approach. In this regard, information on metabolism, gene clusters and TFs involved in the catabolism of selected phenolic acids were analysed. Each identified inducible system was validated by testing its response to the proposed phenolic acid followed by a thorough characterisation. To determine if the inducible system can be applied outside its host strain, the system response was evaluated in the host and/or non-host microorganisms, including well-studied *E. coli*, *C. necator*, and *P. putida*. To enhance the knowledge of biosensor kinetics and dynamics, the dose-response and dynamic range were determined. The specificity of the phenolic acid-biosensors was evaluated against twenty of the most common hydroxybenzoic and hydroxycinnamic acids. Ultimately, the biosensor responding to protocatechuic acid was applied to screening of 4-hydroxybenzoate 3-monooxygenases.

Materials and methods

Chemicals

All chemicals used as inducers in this study are listed in Supplementary Table S4. Stock solutions of inducers were prepared at 100 mM in DMSO (Eurochemicals, Vilnius, Lithuania) and used for serial dilutions in DMSO to obtain desired concentrations.

Bacterial strains and media

All strains employed in this study are listed in Supplementary Table S5. *E. coli* Top10 was used for molecular cloning and vector propagation. Host strains (*E. coli* Top10, *C. necator* H16, and *P. putida* KT2440) were used for biosensors characterisation and were propagated in Luria-Bertani (LB) medium (Fisher Scientific, Pittsburgh, USA) to perform fluorescence and absorbance measurements. Antibiotics were added when required at the following concentrations: 25 μg/mL chloramphenicol for *E. coli*, 50 μg/mL chloramphenicol for *C. necator*, and 12.5 μg/mL tetracycline for *P. putida* KT2440. 15 g/L of agar was added for solid media preparation.

Cloning and transformation

Microbial genomic DNA was obtained using the GenElute Bacterial Genomic DNA Extraction Kit (Sigma-Aldrich, St. Louis, USA). Plasmid DNA was purified employing the GeneJET Plasmid Miniprep Kit (Thermo Fisher Scientific, Vilnius, Lithuania). DNA was amplified by PCR in 20 μl reactions using the Phusion High-Fidelity DNA polymerase (Thermo Fisher Scientific, Vilnius, Lithuania). The Gel DNA Recovery Kit (Zymo Research, Irvine, USA) was used to obtain gel-purified linearised DNA. NEBuilder HiFi DNA Assembly Master Mix was purchased from New England BioLabs (Ipswich, USA), while restriction enzymes, T4 DNA Ligase, and DreamTaq DNA polymerase were purchased from Thermo Fisher Scientific (Vilnius, Lithuania). Oligonucleotide primers were synthesised by Metabion (Planegg, Germany) (Supplementary Table S6). The reactions of PCR, restriction digestion, HiFi DNA Assembly Master Mix followed the manufacturer's protocols. Chemical competent cells of *E. coli* and electrocompetent *C. necator* H16 and *P. putida* KT2440 were prepared and transformed as described previously.

Plasmid construction

Plasmids were constructed using the NEBuilder HiFi DNA Assembly method, validated by colony PCR and restriction-based analysis. The detailed construction of each plasmid is described in Supplementary Methods.

Fluorescence measurements

RFP fluorescence was measured using an Infinite M200 PRO (Tecan, Männedorf, Switzerland) microplate reader with excitation and emission wavelengths set to 585 and 620 nm, and gain factor of 120%. Absorbance was measured at 600 nm wavelength. RFP fluorescence and absorbance were quantified over time, freshly grown bacterial cells were inoculated into 2 mL of LB medium containing the respective antibiotic in 50-mL conical centrifuge tubes and incubated overnight at 30 °C 200 rpm. After incubation, the cultures were diluted to an 0.05–0.1 OD_{600} and grown to 0.15–0.2 OD_{600}, obtaining logarithmically growing cells, which were transferred to a 96-well plate (Corning Incorporated, New York, USA or Thermo Scientific, Waltham, USA) in a 1:50 ratio (adding 142.5 μl of the cell culture and 7.5 μl of the selected inducer, reaching the desired ligand concentration in the well). RFP fluorescence and absorbance values were corrected for autofluorescence and autoabsorbance of the medium, respectively.

Absolute normalised fluorescence values (ANF) were calculated using formula (1).

$$ANF = \frac{RFP_{raw} - RFP_{medium}}{OD_{raw} - OD_{medium}} \quad (1)$$

The system parameters were calculated using the Hill function (2) [12] employing software GraphPad Prism 9.

$$ANF = b_{\max} \times \frac{I^h}{{}^*K_m^h + I^h} + b_{\min} \quad (2)$$

In formula (2): b_{max} and b_{min} – the maximum and minimum levels of RFP synthesis, respectively; I – concentration of inducer; h – the Hill coefficient; $^*K_m$ – the inducer concentration, corresponding to the half-maximal reporter's output.

The dynamic range μ was calculated using formula (3).

$$\mu = \frac{b_{\max}}{ANF_{uninduced}} \quad (3)$$

In formula (3): b_{max} – maximum levels of RFP synthesis; $ANF_{uninduced}$ – absolute normalised fluorescence values of the uninduced sample.

The relative induction values (%) were calculated using the ANF values at a specific inducer concentration in formula (4):

$$Relative \quad normalised \quad fluorescence(\%) = 100 \times \left(\frac{ANF - b_{\min}}{b_{\max}}\right) \quad (4)$$

4-Hydroxybenzoate 3-monooxygenase variants screening

To screen potential 4-hydroxybenzoate 3-monooxygenase variants from species *C. necator*, *B. multivorans, P. aeruginosa* , *P. lactis*, *A. baylyi*, *C. glutamicum,* and *Sphingobium* sp., corresponding plasmids pEA035-pEA041 carrying *pobA*-like genes (locus tags *H16_RS30120, NP80_RS03580, PA0247, TX24_18430, ACIAD1719, CGTRNA_RS05390, E2598_04620*, respectively) placed under control of L-arabinose-inducible system AraC/P_{araBAD} were assembled. In additions, the plasmid pEA034 without *pobA*-like gene was assembled as a negative control. All constructs also included the protocatechuate-inducible system *Ab*PcaU^{AM}/P_{3B5}. A detailed assembly description of plasmids is provided in the Supplementary Methods. Absolute normalised fluorescence of *E. coli* Top10 cells harbouring plasmids pEA034-pEA041 was determined as

described above. Cell cultures were supplemented with either 5 mM *p*-hydroxybenzoate or 5 mM *p*-hydroxybenzoate and 1 mM L-arabinose.

HPLC analysis

HPLC analyses were performed with an Ultimate 3000 HPLC system coupled to a photodiode array (UV–VIS) detector (Thermo Fisher Scientific, Waltham, USA). Chromatographic separation was achieved with a Phenomenex Luna 5 μm C18(2) 100 Å (150 × 4.6 mm) column (Phenomenex, Torrance, USA) equipped with a security guard column, thermostated at 25 °C. The mobile phase A was aqueous 0.1% formic acid (v/v); and mobile phase B was HPLC grade acetonitrile. The elution gradients used were as follows: from 0 until 15 min from 10% to 50% B, from 15 to 17.5 min raised at 70% B; 17.5–20 min decreased to 10% B then kept constant for 2 min. A constant flow rate of 1 mL/min was kept throughout the analysis with the detection wavelength set at 260 nm. The samples were filtered using a 0.22 μm syringe filter. Ten microliters of sample were injected, and chromatograms were recorded and analysed using Chromeleon 7 (Thermo Fisher Scientific, Waltham, USA).

Results

Identification of phenolic acid-inducible gene expression systems

Bacteria have adapted to their living environment by developing rapid response mechanisms to intracellular and extracellular changes. Generally, an inducible gene expression system, composed of an inducible promoter and TF, is used to control the expression of catabolic genes responsible for the metabolite utilisation. In this context, the TF can form a complex with a metabolite, referred as an effector or ligand. Depending on the TF type, such complexes can trigger two alternative modes of action resulting in the activation of gene expression. An activator-type TF in complex with the effector binds specific DNA motif (s) usually located upstream to the core promoter and stimulates the formation of RNA polymerase-promoter complex resulting in the transcriptional initiation (Fig. 1a). A repressor-type TF binds DNA motif(s) located downstream to or within the core promoter sequence and represses the transcription in the absence of the effector (Fig. 1b). The transcription is activated when the TF forms DNA-binding-inactive complex with the effector molecule. Inducible systems involving activator or repressor TF are increasingly applied for the development of biosensors [13–15].

To build a library of putative inducible systems responding to phenolic acids, we, first, examined available information on catabolic pathways (KEGG Pathway Database, www.genome.jp/kegg/pathway.html [16]) and enzymes (BRENDA, www.brenda-enzymes.org [17] and MetaCyc, https://metacyc.org [18]) involved in the bacterial metabolism of these compounds. As summarised in Fig. 2, catabolic pathways have been identified for at least fifteen major phenolic acids in different species of bacteria. Then, we searched for the gene expression systems activated by these compounds amongst previously characterised or proposed systems in the literature (Supplementary Table S1), and identified putative inducible systems in the GenBank database (NCBI, www.ncbi.nlm.nih.gov [19]) by searching for gene clusters composed of

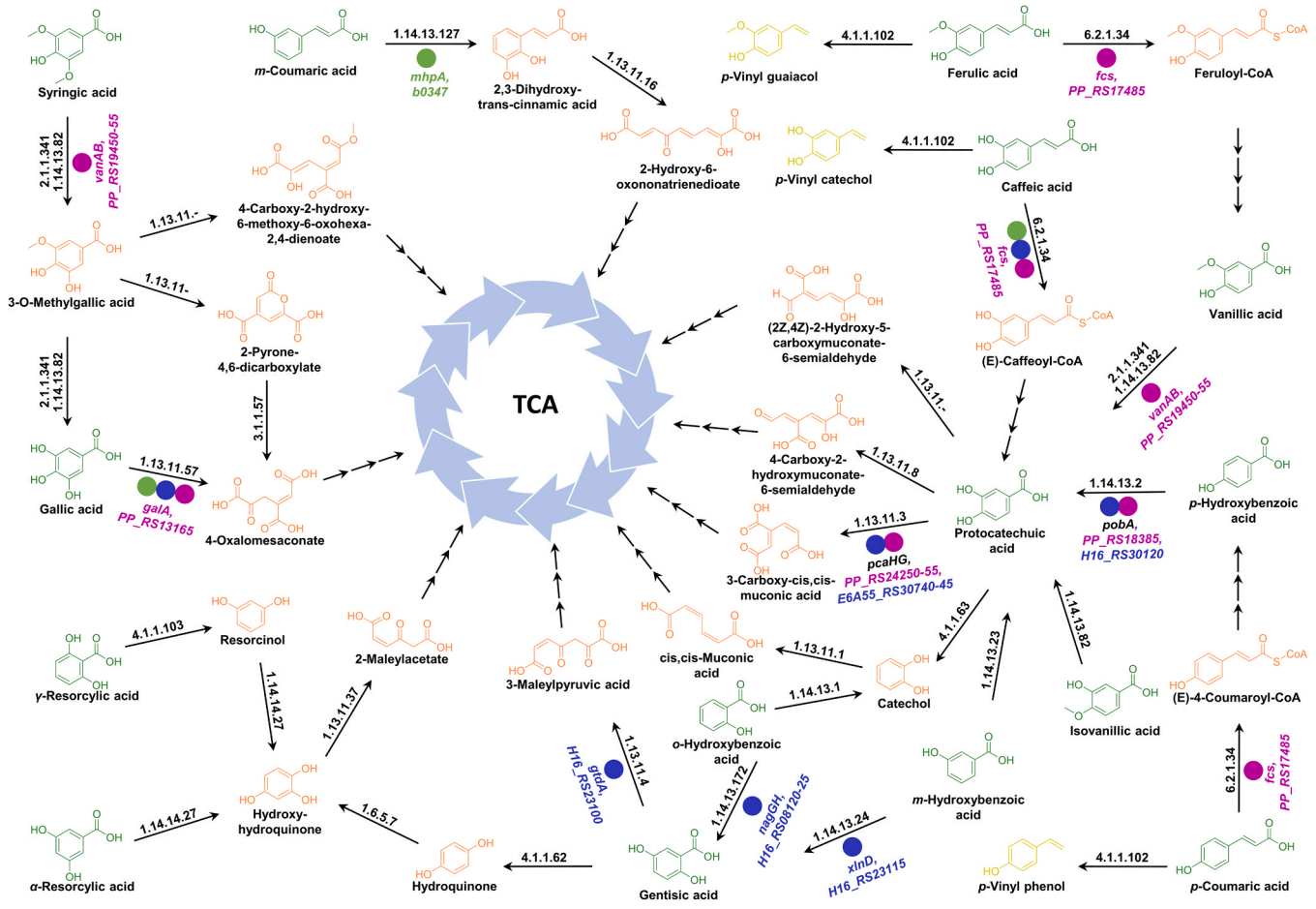

Fig. 1. Schematic representation of (a) activator and (b) repressor TF-based inducible systems. (a) The effector molecule binds to the TF and it allows the active RNA polymerase-promoter complex formation in conjunction initiation of the RFP synthesis. (b) TF binds to the promoter region and inhibits the formation of RNA polymerase-promoter complex, effector molecule inhibits repression by binding to TF, and then TF dissociates from the DNA, and allow RFP transcription.

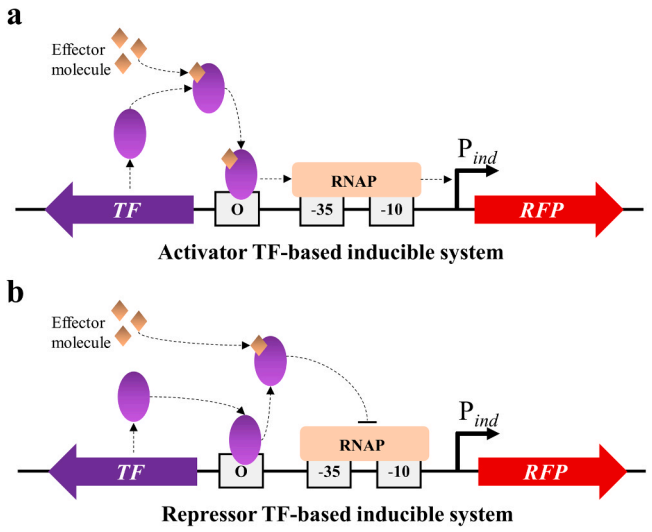

Fig. 2. Bacterial catabolism of phenolic acids. Major phenolic acids, intermediate metabolites towards the TCA cycle, and other compounds are shown in green, orange and yellow, respectively. EC enzyme numbers are indicated above the arrows and dashed arrows indicate several metabolism reactions. The circles and genes names with locus tags under the arrows indicate *E. coli* MG1665 (green), *C. necator* H16 (blue) and *P. putida* KT2440 (purple) respective genes .

genes encoding enzymes involved in phenolic acid transformation and associated TFs as described previously [20]. Identified putative phenolic acid-inducible gene expression systems with relevant gene clusters, composed of one or more functional genes that encode enzymes with catalytic functions and involved in metabolic pathways along with adjacent TF-encoding genes, are presented in Supplementary Fig. S1. Twenty seven inducible systems from *Alphaproteobacteria* (*Caulobacter crescentus* CB15N, *Sphingobium* sp. Leaf26, *Novosphingobium aromaticivorans* DSM12444), *Betaproteobacteria* (*Burkholderia multivorans* ATCC BAA-247, *Cupriavidus necator* H16, *Comamonas testosteroni* ATCC 11996, *Thauera aromatica* DSM 11528), *Gammaproteobacteria* (*Escherichia coli* MG1655, *Acinetobacter baylyi* ADP1, *Pseudomonas aeruginosa* PAO1, *Pseudomonas putida* KT2440), *Actinobacteria* (*C. glutamicum* ATCC13032 and *Rhodococcus jostii* RHA1) or *Bacilli* (*Bacillus megaterium* DSM319 and *Bacillus pumilus* ATCC 7061) were taken forward for further investigation (Table 1 and Supplementary Table S2).

Five previously characterised and optimised TF-based biosensors were selected for further evaluation. These included sensors responding to *o*-hydroxybenzoic acid (1): *Cn*NahR/$P_{H16\_RS08125}$ (LysR family TF, from *C. necator* H16 [20]); vanillic acid (4): *Cc*VanR^{AM}/P_{vanCC} (GntR, *C. crescentus* CB15N [21–23]); protocatechuic acid (7): *Cn*PcaQ/P_{pcaH} (LysR, *C. necator* H16 [20]) and *Ab*PcaU^{AM}/P_{3B5} (IclR, *A. baylyi* ADP1 [22,24]); *p*-coumaric acid (17) and ferulic acid (18): *Ab*HcaR/$P_{A\text{-}CIAD\_RS07960}$ (MarR, *A. baylyi* ADP1 [25]) (Table 1 and Supplementary Table S1).

Nine TF-inducible promoter pairs were identified from the literature search and further examination of available information on catabolic pathways and relevant gene clusters. These inducible systems were predicted to respond to the following phenolic acids: *p*-hydroxybenzoic acid (3): *Ab*PobR/P_{pobA} (IclR family TF, *A. baylyi* ADP1 [26]); gentisic acid (9): *Bm*GtdR/P_{gtdA} (LysR, *B. multivorans* DSM 13243), *Cn*GtdR/P_{gtdA} (LysR, *C. necator* H16), and *Pa*GtdR/P_{gtdA} (LysR, *P. aeruginosa* PAO1), all three reviewed in [27]; *Ct*GenRLysR/$P_{CTATCC11996\_10848}$ (MarR and LysR, *C. testosteroni* ATCC 11996 [28]) and *Cg*GenR/$P_{Cgl3023}$ (IclR, *C. glutamicum* ATCC 13032 [29]); α-resorcylic acid (10): *Ta*DbdR/P_{dbhL} (LysR, *T. aromatica* AR-1 [30]); γ-resorcylic acid (12): *Rj*TsdR/P_{tsdB} (IclR, *R. jostii* RHA1[231]); *m*-coumaric acid (16): *Ec*MhpR/P_{mhpA} (IclR, *E. coli* MG1655 [32]) (Table 1 and Supplementary Table S2).

Moreover, eleven TF homologous of previously reported inducible systems, were identified through multiple genome analysis. These TFs in combination with corresponding were proposed to form inducible systems that can potentially respond to *m*-hydroxybenzoic acid (2): *Ct*MobR/P_{mobA} (MarR family TF, *C. testosteroni* ATCC 11996 homologue of *C. testosteroni* KH122–3 s MobR [33]; *p*-hydroxybenzoic acid (3): *Cn*PobR/P_{pobA} (AraC/XylS, *C. necator* H16 homologue of *A. chroococcum* ATCC 9043 PobR [34]); vanillic acid (4): *Pp*VanR/P_{vanA} (GntR, *P. putida* KT2440 homologue of *C. crescentus* CB15N GntR [21]); vanillic acid (4) and syringic acid (8): *Sp*SyrR/P_{desA} (IclR, *Sphingobium* sp. Leaf26 homologue of *Sphingobium* sp. SYK-6 DesR [335]); gallic acid (6): *Bm*GalR/$P_{NP80\_RS00205}$ (LysR, *B. multivorans* ATCC BAA-247 homologue of *P. putida* KT2440 GalR [36]); syringic acid (8): *Na*DesR/$P_{SARO\_RS12095}$ (IclR, *N. aromaticivorans* DSM12444 homologue of *Sphingobium* sp. SYK-6 DesR [35]); *m*-coumaric acid (16): *Ct*McuR/P_{mhpA} (IclR, *C. testosteroni* ATCC 11996 homologue of *C. testosteroni* TA441 McuR [37]); *p*-coumaric acid (17) and ferulic acid (18): *Bm*PadR/$P_{BMD\_RS01890}$ and *Bp*PadR/$P_{BPUM\_RS03685}$ (PadR, *B. megaterium* DSM319 and *B. pumilus* ATCC 7061 homologues of *B. subtilis* subsp. *subtilis* str. 168 PadR [38]), and *Pp*HcaR/$P_{PP\_RS17495}$ and *Sp*HcaR/P_{ASE85_21485} (MarR, *P. putida* KT2440 and *Sphingobium sp.* Leaf26 homologues of *A. baylyi* ADP1 MarR [25] and *P. fluorescens* BF13 MarR [39], respectively) (Table 1 and Supplementary Tables S1 and S2).

Furthermore, the putative isovanillic acid (5) inducible system *Ct*IvaRVanR/P_{vanA} (MarR and GntR family TFs, *C. testosteroni* ATCC 11996) was predicted by the protein homology analysis using a previously determined gene cluster associated with the metabolism of isovanillic acid, vanillic acid, and veratric acid in *Comamonas testosteroni* strain BR6020 (Supplementary Table S2) [40]. Finally, the gallic acid (6) inducible system *Pp*GalR/P_{galT} was designed using the LysR family TF GalR [36] and the upstream promoter region of the *galT* gene of *P. putida* KT2440 (Table 1).

Validation and evaluation of inducible systems

To validate systems response to the target phenolic acids, all identified putative inducible systems (Supplementary Table S2) were assembled in a fluorescence reporter vector as described in [41] and Supplementary Methods (Supplementary Information). First, the plasmids constructs carrying these systems were introduced into *E. coli*. The resulting strains were grown in rich Luria-Bertani (LB) medium and the absolute normalised fluorescence of the logarithmically growing cells was quantified 6 h after extracellular supplementation with the corresponding phenolic acid to a final concentration of 5 mM (Fig. 3 and Supplementary Fig. S2). Of the twenty seven putative phenolic acid-inducible systems (Supplementary Table S2), ten showed a significant activation in *E. coli* (Fig. 3c and Supplementary Fig. S2b) when growth medium was supplemented with the corresponding proposed phenolic acids.

However, other putative inducible systems exhibited no significant activation in *E. coli* (Fig. 3c, Supplementary Figs. S2b). We hypothesised that either: 1) the efficiency of heterologous expression is limited and TF required for inducible system regulation is not produced in *E. coli*, 2) the phenolic acid uptake is restricted in *E. coli* or 3) systems are activated by metabolic intermediate of proposed primary inducer, which is not produced in non-host bacterium. To test these hypotheses and to investigate if these limitations can be resolved by using alternative hosts, all putative inducible systems were subjected to evaluation using *C. necator* H16 and *P. putida* KT2440. These bacterial species are known to possess relatively well-developed metabolism of phenolic acids, ensuring the uptake of phenolic compounds and enabling the generation of intermediates required for induction. Moreover, they are native hosts for some of these inducible systems.

C. necator strains harboring the putative gentisic acid-inducible systems from *B. multivorans* DSM 13243, *P. aeruginosa* PAO1 and *C. necator* H16 mediated a significant increase in RFP synthesis after

Table 1
Putative phenolic acid-inducible gene expression systems investigated in this work.

No	Phenolic acid	Inducible system	Regulator	Regulator locus tag	Regulator family	Promoter	Source	References	Constructs	
									TR and promoter	Promoter only
1	*o*-hydroxybenzoic acid (1)	*Cn*NahR/ $P_{H16\_RS08125}$	NahR	*H16_RS08130*	LysR	$P_{H16\_RS08125}$	*C. necator* H16	[20]	pEH042	pEH095
2	*m*-hydroxybenzoic acid (2)	*Ct*MobR/P_{mobA}	MobR	*CT4_RS21125*	MarR	P_{mobA}	*C. testosteroni* ATCC 11996	this study, homologue [33]	pEV019	pEV020
3	*p*-hydroxybenzoic acid (3)	*Cn*PobR/P_{pobA}	PobR	*H16_RS30125*	AraC/XylS	P_{pobA}	*C. necator* H16	this study, homologue [34]	pEV021	pEV022
4	*p*-hydroxybenzoic acid (3)	*Ab*PobR/P_{pobA}	PobR	*ACIAD_RS07920*	IclR	P_{pobA}	*A. baylyi* ADP1	[26]	pEV031	pEV032
5	vanillic acid (4)	*Cc*VanR^{AM} /P_{vanCC}	VanR^{AM}	*CCNA_02475*	GntR	P_{vanCC}	*C. crescentus* (available in addgene pAJM.773)	[22]	pIJ015	N/A
6	vanillic acid (4)	*Pp*VanR/P_{vanA}	VanR	*PP_RS19460*	GntR	P_{vanA}	*P. putida* KT2440	this study, homologue [21]	pIJ003	pIJ001
7	gallic acid (6)	*Pp*GalR/P_{galT}	GalR	*PP_RS13155*	LysR	P_{galT}	*P. putida* KT2440	this study, homologue [36]	pEV005	pEV005A
8	protocatechuic acid (7)	*Ab*PcaU^{AM}/ P_{3B5}	PcaU^{AM}	*ACIAD_RS07845*	IclR	P_{3B5}	*A. baylyi* ADP1 (available in addgene pAJM.690)	[22]	pIJ018	N/A
9	protocatechuic acid (7)	*Cn*PcaQ/P_{pcaH}	PcaQ	*H16_RS30150*	LysR	P_{pcaH}	*C. necator* H16	[20]	pEH161	pEH171
10	gentisic acid (9)	*Bm*GtdR/P_{gtdA}	GtdR	*NP80_RS07200*	LysR	P_{gtdA}	*B. multivorans* DSM 13243	[27]	pIK016	pIK015
11	gentisic acid (9)	*Cn*GtdR/P_{gtdA}	GtdR	*H16_RS23095*	LysR	P_{gtdA}	*C. necator* H16	[27]	pEV004	pEV004A
12	gentisic acid (9)	*Pa*GtdR/P_{gtdA}	GtdR	*PA2469*	LysR	P_{gtdA}	*P. aeruginosa* PAO1	[27]	pEV003	pEV003A
13	α-resorcylic acid (10)	*Ta*DbdR/P_{dbhL}	DbdR	N/A	LysR	P_{dbhL}	*T. aromatica* DSM 11528	[30]	pEA054	pEA045
14	*m*-coumaric acid (16)	*Ec*MhpR/ P_{mhpA}	MhpR	*b0346*	IclR	P_{mhpA}	*E. coli* MG1655	[32]	pEV052	pEV053
15	*p*-coumaric acid (17) and ferulic acid (18)	*Bm*PadR/ $P_{BMD\_RS01890}$	PadR	*BMD_RS02905*	PadR	$P_{BMD\_RS01890}$	*B. megaterium* DSM 319	this study, homologue [38]	pIK010	pIK008
16	*p*-coumaric acid (17) and ferulic acid (18)	*Bp*PadR/ $P_{BPUM\_RS03685}$	PadR	*BPUM_RS03690*	PadR	$P_{BPUM\_RS03685}$	*B. pumilus* ATCC 7061	this study, homologue [38]	pIK002	pIK001
17	*p*-coumaric acid (17) and ferulic acid (18)	*Pp*HcaR/ $P_{PP\_RS17495}$	HcaR[a]	*PP_RS17500*	MarR	$P_{PP\_RS17495}$	*P. putida* KT2440	this study, homologue [25]	pEV040	pEV041
18	*p*-coumaric acid (17) and ferulic acid (18)	*Ab*HcaR/ $P_{ACIAD\_RS07960}$	HcaR[a]	*ACIAD_RS07970*	MarR	$P_{ACIAD\_RS07960}$	*A. baylyi* ADP1	[25]	pEV035	pEV036

N/A – not available; a – regulator abbreviation given by the authors

inducer addition (Fig. 3d and Supplementary Fig. S2c). Whereas in *P. putida* (Fig. 3e and Supplementary Fig. S2d), the expression of the reporter gene was significantly activated for the gallic acid-inducible and *p*-coumaric acid-inducible systems, both originating from the host. Similarly, *P. putida* harbouring the *p*-coumaric acid-inducible system from *A. baylyi* ADP1 exhibited increased RFP synthesis. The vanillic acid-inducible system from *P. putida* KT2440 and α–resorcylic acid-inducible system from *T. aromatica* DSM 11528 were activated in both *C. necator* and *P. putida*. Altogether, eight inducible systems exhibited response to target phenolic acids in *C. necator*, *P. putida* or both, but not in *E. coli*.

Eight systems responded to the target phenolic acids in at least two different bacterial species, whereas fourteen of eighteen systems were induced in at least one species of different genus. This indicates the broad-host-range applicability of the studied phenolic acid-inducible systems. It should be noted that we report here for the first time an inducible system responding to the gentisic acid. However, it is not clear why the activation of gene expression by this compound was only observed in *C. necator* (Fig. 3d). Further research will be required to elucidate the biological basis of this phenomenon.

However, eight putative inducible systems exhibited no response to target phenolic acids (Supplementary Table S2). Two putative syringic acid-inducible systems from GC-rich *Sphingobium sp.* Leaf26 (*Sp*SyrR/ P_{desA}) and *N. aromaticivorans* DSM12444 (*Na*DesR/$P_{SARO\_RS12095}$) showed no induction (data not shown), even though their proposed inducer is likely to be uptaken by bacterial strains used in this study. Likewise, putative inducible system from *Sphingobium sp.* Leaf26 did not respond to *p*-coumaric acid, despite that the homologous systems from *Betaproteobacteria* were activated by this compound. Among the systems that did not respond to the proposed inducer were also two putative gentisic acid-inducible systems from *C. testosteroni* ATCC 11996 and *C. glutamicum* ATCC 13032. Differently from the other three gentisic acid-inducible systems controlled by LysR-type regulators, these systems were arranged with non-typical TF, LysR-MarR pair, and IclR, respectively.

The only system proposed to respond to γ-resorcylic acid, the *Rj*TsdR/P_{tsdB}, exhibited no activation of gene expression in either of the three bacterial strains used in this study. However, the promoter only

version mediated approximately 400-fold higher RFP synthesis in *P. putida* than the system composed of TF and promoter (Supplementary Fig. S3). This not only confirmed that TsdR acts as a transcriptional repressor [31], but also indicated that the *tsdR* gene was expressed and the regulatory elements of P_{tsdB} were functional in *P. putida*. Previously, the γ-resorcylic acid has been shown to interact with TsdR by inhibiting its binding to *tsdR-tsdB* intergenic region [31]. Consequently, the lack of induction in *P. putida* can potentially be attributed to the limited uptake of γ-resorcylic acid by this bacterium. Notably, neither *E. coli*, *C. necator*, or *P. putida* exhibited any catabolic activity on γ-resorcylic acid. The putative isovanillic acid- and gallic acid-inducible systems *Ct*IvaRVanR/P_{vanA} and *Bm*GalR/$P_{NP80\_RS00205}$ showed no response to target phenolic acids in *E. coli*, *C. necator* or *P. putida* (data not shown). Further research is required to elucidate the mechanism underlying the activation of these systems.

Verification and function of TFs

A TF can activate or repress the gene expression from the inducible promoter. It forms a complex with a characteristic DNA sequence, the operator, and facilitates or hinders the RNA-polymerase binding to the promoter. The TF-operator complex formation can depend on the presence of the inducer that binds to the regulator and by changing its conformation enhances or reduces the TF affinity to the operator sequence (Fig. 1). To verify the role and function of TFs assigned to inducible systems, the reporter gene expression level of constructs carrying TF with inducible promoter was compared to that of constructs with the promoter only (Fig. 3 and Supplementary Fig. S2 *versus* Supplementary Figs. S4 and S5; Supplementary Figs. S6 and S7 *versus* Supplementary Figs. S8 and S9). With exception of *Bm*GtdR/P_{gtdA} and *Cn*NahR/$P_{H16\_RS08125}$, the induction level was negligible or significantly reduced when the TF gene was excluded in all inducible systems that were shown to mediate the activation of gene expression in the presence of target phenolic acid (Supplementary Fig. S4). In those cases, where

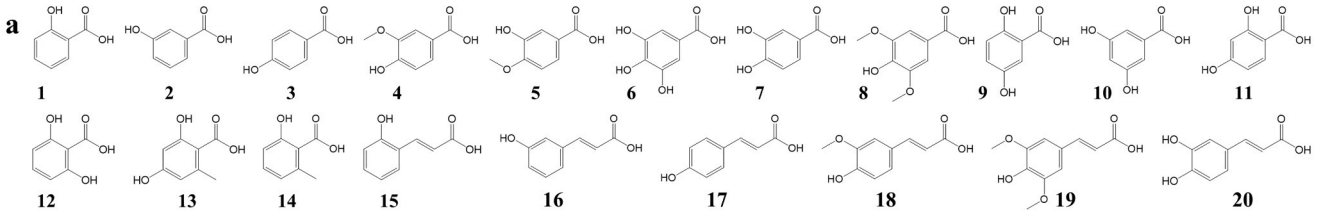

b

Phenolic acid	Source	Inducible system
o-hydroxybenzoic acid (1)	*C. necator* H16	*Cn*NahR/$P_{H16\_RS08125}$
m-hydroxybenzoic acid (2)	*C. testosteroni* ATCC 11996	*Ct*MobR/P_{mobA}
p-hydroxybenzoic acid (3)	*C. necator* H16	*Cn*PobR/P_{pobA}
vanillic acid (4)	*C. crescentus*, pAJM.773	*Cc*VanR^{AM}/P_{vanCC}
gallic acid (6)	*P. putida* KT2440	*Pp*GalR/P_{galT}
protocatechuic acid (7)	*A. baylyi* ADP1, pAJM.690	*Ab*PcaU^{AM}/P_{3B5}
gentisic acid (9)	*B. multivorans* DSM 13243	*Bm*GtdR/P_{gtdA}
α-resorcylic acid (10)	*T. aromatica* DSM 11528	*Ta*DbdR/P_{dbhL}
m-coumaric acid (16)	*E. coli* MG1655	*Ec*MhpR/P_{mhpA}
p-coumaric acid (17)	*B. megaterium* DSM 319	*Bm*PadR/$P_{BMD\_RS01890}$
ferulic acid (18)	*B. megaterium* DSM 319	*Bm*PadR/$P_{BMD\_RS01890}$

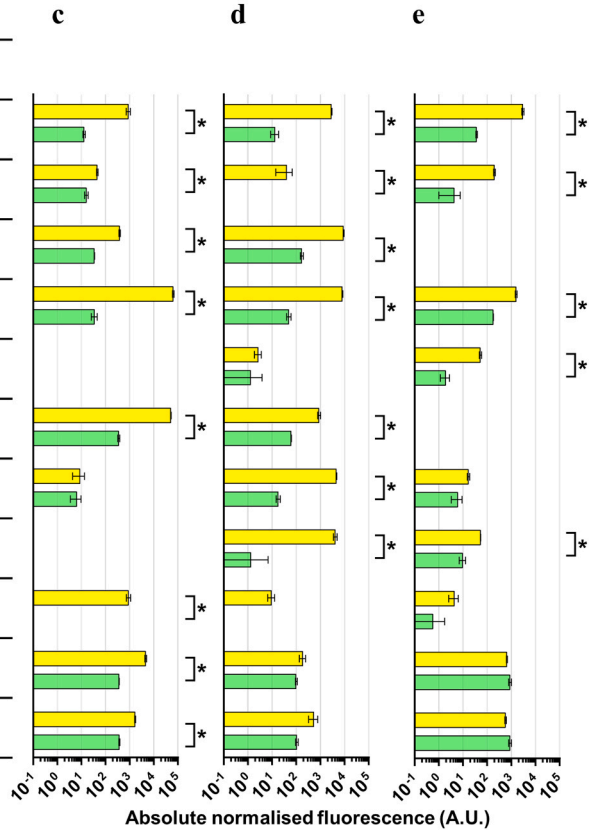

Fig. 3. Evaluation of phenolic acid-biosensors. (a) Chemical structures of selected phenolic acids: *o*-hydroxybenzoic acid (1), *m*-hydroxybenzoic acid (2), *p*-hydroxybenzoic acid (3), vanillic acid (4), isovanillic acid (5), gallic acid (6), protocatechuic acid (7), syringic acid (8), gentisic acid (9), α-resorcylic acid (10), β-resorcylic acid (11), γ-resorcylic acid (12), orsellinic acid (13), 6-methylsalicylic acid (14), *o*-coumaric acid (15), *m*-coumaric acid (16), *p*-coumaric acid (17), ferulic acid (18), sinapic acid (19), and caffeic acid (20). (b) Summary of the identified systems activated by phenolic acids. (c-e) Single time-point absolute normalised fluorescence measured using *E. coli*, *C. necator* and *P. putida*, respectively, harbouring plasmids with the TF-based inducible gene expression systems as indicated in the panel (b). Fluorescence output was determined 6 h after extracellular supplementation with the corresponding phenolic acid to a final concentration of 5 mM (in yellow) and in the absence of inducer (in green). Error bars represent standard deviations of three biological replicates. Asterisks indicate statistically significant differences between the fluorescence output of the uninduced and induced sample (* $p < 0.001$; unpaired *t*-test).

the promoter only construct was assayed in the organism it originated from, the promoter activity under induced condition remained almost unaltered due to availability of the TF copy encoded in the host genome. Surprisingly, promoter only construct containing *Bm*P_{gtdA} from *B. multivorans* DSM 13243 and lacking the copy of the TF gene *gtdR*, mediated the activation of gene expression in the presence of gentisic acid in *C. necator* (Supplementary Fig. S4c). This indicates that the promoter *Bm*P_{gtdA} can be activated by unknown TF specific to this host. As shown previously [20], the inducible promoter *Cn*$P_{H16\_RS08125}$ was activated by *o*-hydroxybenzoic acid in *P. putida* despite the absence of the corresponding TF gene *nahR* (Supplementary Fig. S4d). For all inducible systems (Fig. 3 and Supplementary Fig. S2), the assigned TFs responded to the presence of target phenolic acids and they were essential to regulate the gene expression from corresponding inducible promoters, as predicted in this study or proposed previously (Supplementary Table S1).

A few 'promoter only' constructs including *Ct*P_{mobA}, *Pp*P_{vanA}, *Bm*$P_{BMD\_RS01890}$, *Bp*$P_{BPUM\_RS03685}$, and *Ab*$P_{ACIAD\_RS07960}$ exhibited a greater RFP synthesis under uninduced condition than that of inducible systems *Ct*MobR/P_{mobA}, (responding to *m*-hydroxybenzoic acid), *Pp*VanR/P_{vanA} (vanillic acid), *Bm*PadR/$P_{BMD\_RS01890}$, *Bp*PadR/$P_{BPUM\_RS03685}$, and *Ab*HcaR/$P_{ACIAD\_RS07960}$ (all three to *p*-coumaric/ferulic acid), respectively. Whereas *Pp*$P_{PP\_RS17495}$ exhibited similar level of reporter gene expression to that of *Pp*HcaR/$P_{PP\_RS17495}$ under an uninduced condition in *P. putida* due to the presence of *hcaR* copy in the host genome. Altogether, this shows that TFs from *m*-hydroxybenzoic, vanillic, and *p*-coumaric/ferulic acid-inducible systems act as transcriptional repressors and their assigned function is in an agreement with earlier studies on corresponding systems or their homologues [23,25,33,42] (Supplementary Table S1). All other regulators from *o*-hydroxybenzoic, *p*-hydroxybenzoic, gallic, protocatechuic, gentisic, *α*-resorcylic and *m*-coumaric acid-inducible systems can be assigned to activators or dual-function TFs.

Characterisation of biosensors

Operational and dynamic range of eighteen biosensors responding to different phenolic acids (Fig. 3 and Supplementary Fig. S2) were evaluated in either *E. coli*, *C. necator*, or *P. putida* strain background. The fastest kinetics of induction (Supplementary Figs. S6 and S7) and the highest dynamic range were main determinants used to choose optimal chassis between these three bacteria (Fig. 3, Supplementary Fig. S2). *E. coli*, *C. necator*, and *P. putida*-based biosensors were grown in LB medium and reporter gene expression was monitored after supplementation with inducer of concentrations from 0 to 5 mM. The dose-response curve was obtained by plotting the relative normalised fluorescence values (%) as a function of inducer concentrations 6 or 12 h after phenolic acid addition (Fig. 4, Supplementary Fig. S10). Parameters including operational and dynamic range, $^*K_m$ value and Hill coefficient were determined from the dose-response curve (Table 2, Supplementary Table S3).

The *E. coli*-based biosensor containing the *Ec*MhpR/P_{mhpA}-inducible system exhibited the highest 1769-fold activation in response to *m*-coumaric acid with the gene expression tunable in the concentration range from 9.7 μM to 5 mM (Fig. 4, Table 2). Similarly, the *E. coli*-based vanillic acid-sensor with *Cc*$VanR^{AM}$/P_{vanCC} showed one of the highest

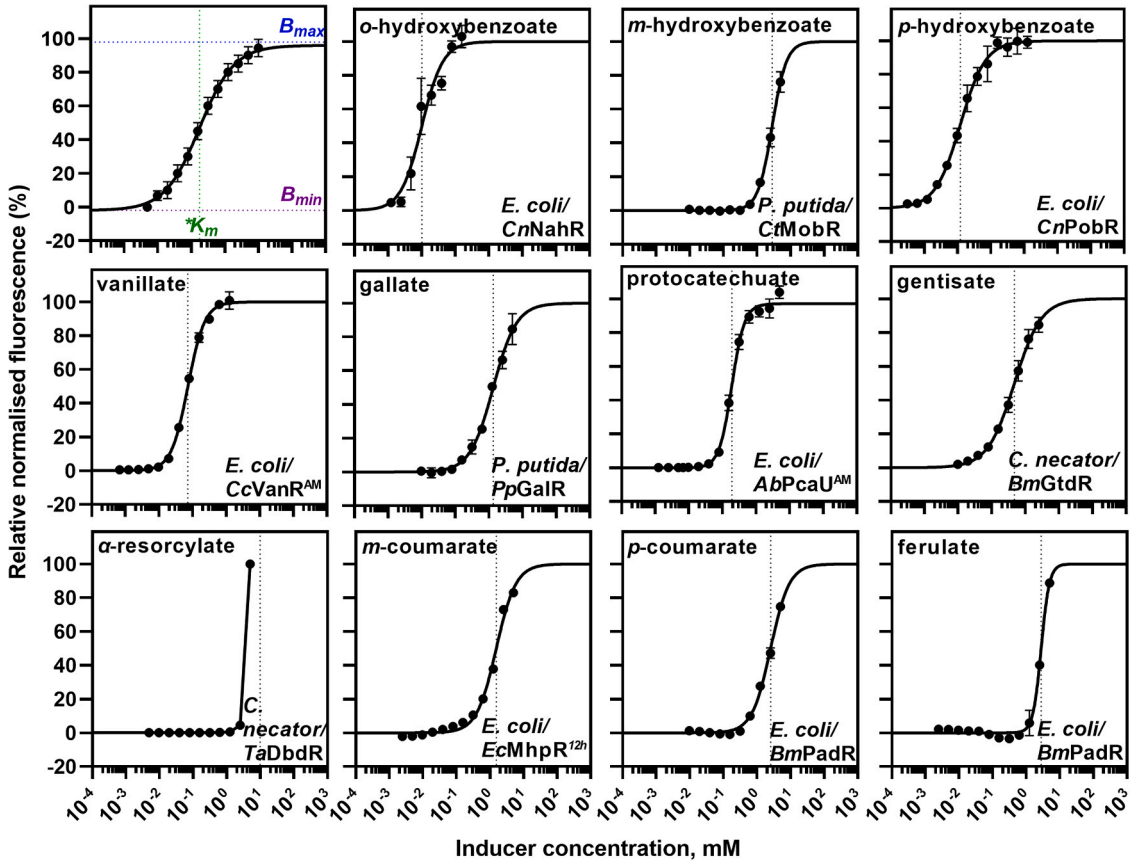

Fig. 4. Dose–response curves of phenolic acid-biosensors. Relative normalised fluorescence (%) of *E. coli*, *C. necator*, and *P. putida* harbouring phenolic acids inducible system–reporter constructs determined in response to different concentrations of respective phenolic acid 6 h or 12 h (indicated-$^{12\,h}$) after inducer addition. Level range of phenolic acids varied from 0 to 5 mM. The dose–responses were fit using a Hill function (see Materials and methods). The maximum level of reporter output b_{max} was set to 100%. The inducer concentration that mediates half-maximal reporter output $^*K_m$ is indicated by a dotted line. Error bars represent standard deviations of three biological replicates.

Table 2
Parameters of the phenolic acid-biosensors.

Inducible system	Application host	Inducer	Dynamic range, in -fold[a]	Operational range, mM	$*K_m$, mM	Hill coefficient
*Cn*NahR/$P_{H16\_RS08125}$	*E. coli* Top10	*o*-hydroxybenzoic acid	19.31 ± 1.12	0.0024–0.156	0.010 ± 0.002	1.63 ± 0.05
*Ct*MobR/P_{mobA}	*P. putida* KT2440	*m*-hydroxybenzoic acid	83.22 ± 44.37	0.3125–5	2.894 ± 0.388	2.04 ± 0.11
*Cn*PobR/P_{pobA}	*E. coli* Top10	*p*-hydroxybenzoic acid	8.67 ± 0.34	0.0006–0.156	0.012 ± 0.002	1.17 ± 0.12
*Cc*VanR^{AM}/P_{vanCC}	*E. coli* Top10	vanillic acid	1293.88 ± 61.02	0.0097–1.25	0.074 ± 0.003	1.83 ± 0.04
*Pp*GalR/P_{galT}	*P. putida* KT2440	gallic acid	34.66 ± 8.92	0.039–5	1.716 ± 0.638	1.31 ± 0.39
*Ab*PcaU^{AM}/P_{3B5}	*E. coli* Top10	protocatechuic acid	137.26 ± 3.103	0.0195–5	0.185 ± 0.010	2.35 ± 0.10
*Bm*GtdR/P_{gtdA}	*C. necator* H16	gentisic acid	362.53 ± 47.58	0.0097–2.5	0.487 ± 0.124	1.13 ± 0.10
*Ta*DbdR/P_{dbhL}	*C. necator* H16	*α*-resorcylic acid	ND	ND	ND	ND
*Ec*MhpR/P_{mhpA}	*E. coli* Top10	*m*-coumaric acid	1768.83 ± 34.11	0.0097–5	1.535 ± 0.064	1.53 ± 0.10
*Bm*PadR/$P_{BMD\_RS01890}$	*E. coli* Top10	*p*-coumaric acid	7.66 ± 0.83	0.312–5	2.586 ± 0.344	1.57 ± 0.05
*Bm*PadR/$P_{BMD\_RS01890}$	*E. coli* Top10	ferulic acid	4.77 ± 0.48	0.625–5	2.897 ± 0.326	2.74 ± 0.03

dynamic ranges of 1294-fold in agreement with previous study [22]. Another vanillic acid-biosensor, which contains a VanR homologue with its cognate inducible promoter from *P. putida* KT2440 (*Pp*VanR/P_{vanA}), exhibited comparable dynamics parameters to *Cc*VanR^{AM}/P_{vanCC}-based system. A high dynamic range of 137- and 108-fold manifested protocatechuic acid-biosensors containing *Ab*PcaU^{AM}/P_{3B5} and *Cn*PcaQ/$P_{H16\_RS30145}$ inducible systems, respectively. However, the former exhibits a significantly lower $*K_m$ value (0.185 mM) than the *Cn*PcaQ/$P_{H16\_RS30145}$-based biosensor (1.286 mM). *p*-Coumaric acid-inducible systems *Ab*HcaR/$P_{ACIAD\_RS07960}$ and *Pp*HcaR/$P_{PP\_RS17495}$ mediated the activation of gene expression exclusively in *P. putida*.

Notably, *E. coli*-based biosensor harbouring inducible system *Cn*NahR/$P_{H16\_RS08125}$ showed a high sensitivity to *o*-hydroxybenzoic acid with the limit of detection of approximately 2.4 μM and $*K_m$ value of approximately 10 μM. Even lower $*K_m$ value of 2 μM has been determined previously when this system has been applied in the native *C. necator* background [20]. *Cn*PobR/P_{pobA} was another system operating in the μM range from 0.6 to 156 μM and $*K_m$ value of 12 μM with *p*-hydroxybenzoic acid in *E. coli* background. An analogous system from *A. baylyi* ADP1 showed a higher $*K_m$ value of 0.279 mM and the range of operation from 19.5 μM to 5 mM. It should be noted that in the case of *Ct*MobR, *Pp*GalR, *Bm*GntR, *Ec*MhpR, *Bm*PadR, *Pp*VanR, *Cn*PcaQ, *Cn*GntR, *Pa*GntR, *Ab*HcaR, and *Bp*PadR, it was only possible to approximate the maximal operational boundary by fitting data, covering effector concentration range up to 5 mM, to Hill function due to a strong growth inhibition at higher concentrations (Supplementary Fig. S11).

Specificity of phenolic acid-biosensors

Inducible gene expression systems respond to various environmental changes, including the availability of nutrient sources. The response is often induced by the TF interaction with a specific chemical compound, the primary inducer, or its metabolic intermediate. Despite the naturally evolved high selectivity, the TFs can interact with compounds that are structurally similar. In this study, the specificity of biosensors was investigated by screening against twenty structurally similar phenolic acids (Fig. 5).

Based on the results of this screen, biosensors containing phenolic acid-inducible systems were divided into three groups. The first group comprises the systems specific to their target phenolic acid and includes

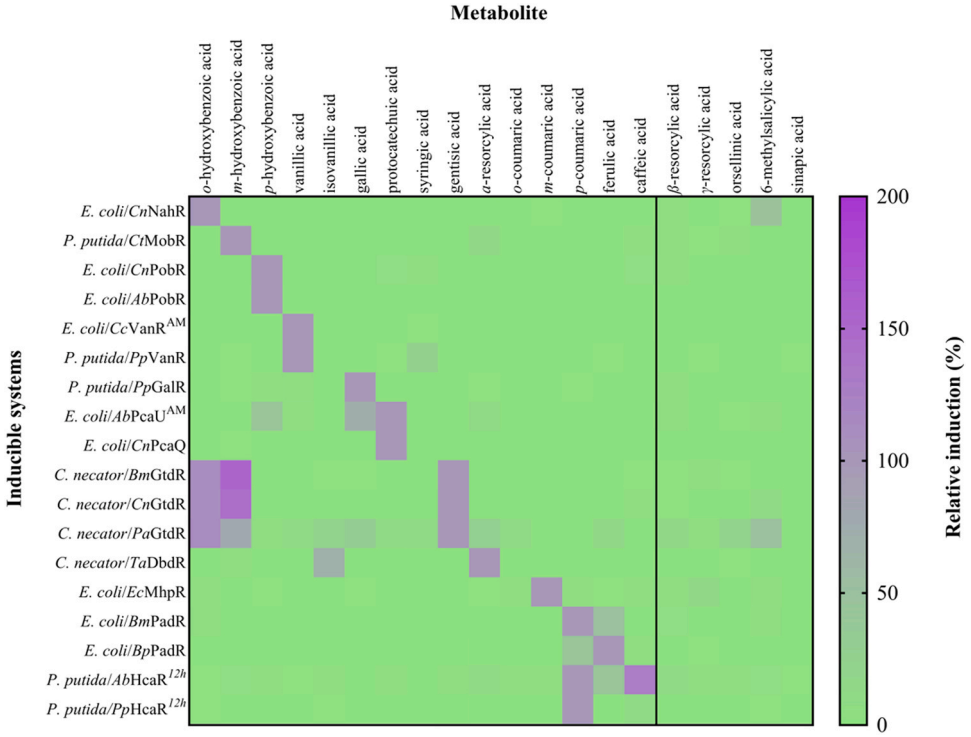

Fig. 5. Evaluation of biosensors' specificity using structurally similar phenolic acids. The heat map illustrates activation of reporter gene expression in the presence of the phenolic acid (in %) relative to the induction mediated by the primary phenolic acid. Measurements were taken 6 h or 12 h (indicated-$^{12\,h}$) after supplementation of inducer at a final concentration of 5 mM. Measurements were performed with three biological replicates.

*Ct*MobR/P_{mobA}, *Cn*PobR/P_{pobA}, *Cc*VanR^{AM}/P_{VanCC}, *Pp*GalR/P_{galT}, *Ec*MhpR/P_{mhpA}, *Bm*PadR/$P_{BMD\_RS01890}$, *Ab*PobR/P_{pobA}, and *Cn*PcaQ/$P_{H16\_RS30145}$.

Another group comprises systems that respond to several structurally similar compounds. For example, *Cn*NahR/$P_{H16\_RS08125}$ system mediated the activation of gene expression in the presence of not only *o*-hydroxybenzoic acid, but also 6-methylsalicylic acid. Whereas the α–resorcylic acid-biosensor (*Ta*DbdR/P_{dbhL}) showed induction with isovanillic acid. Surprisingly, the protocatechuic acid-inducible system *Ab*PcaU^{AM}/P_{3B5} was additionally induced by *p*-hydroxybenzoic acid and gallic acid. We hypothesise that the observed activation by these two compounds is likely imposed by the alteration of PcaU^{AM} structure, the modification of which is detailed in [22].

The systems assigned to the third group respond to metabolically related phenolic acids or metabolites. Besides primary effector, *C. necator* H16-based biosensors harbouring gentisic acid-inducible systems including *Bm*GtdR/P_{gtdA}, *Cn*GtdR/P_{gtdA}, and *Pa*GtdR/P_{gtdA} exhibited activation of gene expression in the presence of *o*-hydroxybenzoic and *m*-hydroxybenzoic acids. This can be explained by the availability of 3-hydroxybenzoate-6-hydroxylase (locus tag *H16_RS23115*) and salicylate-5-hydroxylase (locus tag *H16_RS08125*) in *C. necator* H16, which enables the conversion of *m*-hydroxybenzoic acid and *o*-hydroxybenzoic acid to the primary inducer, the gentisic acid (Fig. 2). Vanillic acid-biosensor containing inducible system *Pp*VanR/P_{vanA} was significantly activated by syringic acid. Likely, the vanillate *O*-demethylase encoded by the *vanA* and *vanB* genes is able catalyse the demethylation of syringic acid as reported in [43] (Fig. 2). The *Bm*PadR/$P_{BMD\_RS01890}$ and *Bp*PadR/$P_{BPUM\_RS03685}$ systems were activated by *p*-coumaric and ferulic acids in *E. coli*. *Bm*PadR/$P_{BMD\_RS01890}$ exhibited a preference for *p*-coumaric acid, whereas *Bp*PadR/$P_{BPUM\_RS03685}$ showed the strongest response to ferulic acid. The gene encoding phenolic acid decarboxylase (PDC) is regulated by PadR TF. PDC can decarboxylate *p*-coumaric, ferulic, and caffeic acids to the corresponding vinyl derivatives (vinylphenol, vinylguaiacol, and vinylcatechol, respectively) (Fig. 2). Surprisingly, these systems did not show induction with caffeic acid in *E. coli*. The other homologues *Ab*HcaR/$P_{ACIAD\_RS07960}$ and *Pp*HcaR/$P_{PP\_RS17495}$ systems exhibited activation by hydroxycinnamic acids. The *Pp*HcaR/$P_{PP\_RS17495}$ did not show induction with ferulic acid, whereas the *A. baylyi* homologue mediated the activation of gene expression in the presence of three hydroxycinnamic acids, *p*-coumaric, ferulic, and caffeic acids. The response is related to the interaction of hydroxycinnamoyl-CoA thioesters ((*E*)-4-coumaroyl-CoA, feruloyl-CoA, and (*E*)-caffeoyl-CoA, respectively) and the HcaR TF as shown previously in [25]. Hydroxycinnamoyl-CoA thioesters are obtained from hydroxycinnamic acids with the participation of the *fcs* gene located in *P. putida* KT2440 genome and encoding the feruloyl-CoA synthetase enzyme (Fig. 2). We accordingly hypothesize that the actual inducers of the *Ab*HcaR/$P_{ACIAD\_RS07960}$ and *Pp*HcaR/$P_{PP\_RS17495}$ systems are not hydroxycinnamic acids, but their hydroxycinnamoyl-CoA thioesters.

Application of protocatechuic acid-biosensor for screening of 4-hydroxybenzoate 3-monooxygenase variants

A 4-hydroxybenzoate 3-monooxygenase (PobA; EC 1.14.13.2) catalyses the conversion of *p*-hydroxybenzoic acid to protocatechuic acid (Fig. 2). Previously, homologues of this enzyme have been characterised in *Pseudomonas* sp., *Rhodococcus* sp., *Acinetobacter* sp, *Cupriavidus necator*, and other bacteria [44,45]. In this study, protocatechuic acid-responsive biosensor was employed for screening of PobA-like variants for their activity to convert *p*-hydroxybenzoic acid into protocatechuic acid. Two inducible systems *Ab*PcaU^{AM}/P_{3B5} and *Cn*PcaQ/$P_{H16\_RS30145}$ were shown to respond to protocatechuic acid. The *Cn*PcaQ/$P_{H16\_RS30145}$-based biosensor exhibited high specificity to protocatechuic acid, whereas *A. baylyi* counterpart showed less stringent selectivity, responding to structurally similar hydroxybenzoic acids in the following order: protocatechuate>gallate> *p*-hydroxybenzoate> α-resorcylate (Fig. 5). We chose to exploit the differential response of this system when the substrate and product of the enzymatic reaction by a PobA-like enzyme was present. It was deemed that a comparably lower level of response to *p*-hydroxybenzoic acid (Fig. 6a) by biosensor would allow a differentiation between substrate and the product providing additional quantitative data for 4-hydroxybenzoate 3-monooxygenase catalysed transformation.

To identify new candidates of 4-hydroxybenzoate 3-monooxygenase, the PobA sequence from *A. baylyi* [26] was applied to search for PobA homologues in *Alphaproteobacteria*, *Betaproteobacteria*, *Gammaproteobacteria*, and *Actinobacteria* using a basic local alignment search tool (BLAST) (https://blast.ncbi.nlm.nih.gov/Blast.cgi) (Fig. 6b). Constructs

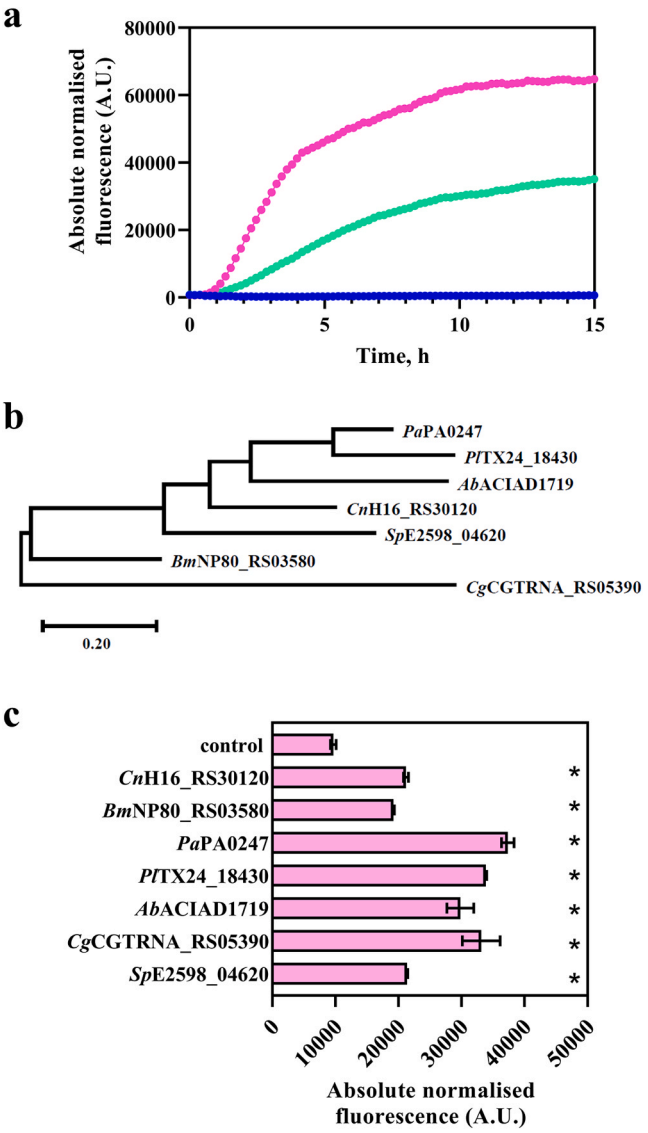

Fig. 6. Biosensor-based screening of naturally occurring bacterial PobA variants. (a) Absolute normalised fluorescence of *E. coli* harbouring the *Ab*PcaU^{AM}/P_{3B5} inducible system based biosensor. RFP-fluorescence output was determined in the absence of inducer (blue) and in the presence protocatechuic acid (pink) and *p*-hydroxybenzoic acid (green), which were added at time 0 h to a final concentration of 5 mM. Cells were grown in LB medium for 15 h. (b) Seven *pobA* variants from different bacteria were chosen for screening of *in vivo* gene activity. Phylogenetic tree was generated using MEGA11 and protein sequence inputs [46]. (c) Absolute normalised fluorescence of *E. coli* Top10 harbouring constructs without *pobA* gene and with putative *pobA* genes. Single time-point fluorescence measurements were taken 6 h after addition of *p*-hydroxybenzoic acid to a final concentration of 5 mM. Error bars represent standard deviations of three biological replicates, * $p \leq 0.01$ (unpaired *t*-test).

pEA035–pEA041 containing the protocatechuic acid biosensor and variants of the *pobA*-like gene from *C. necator*, *B. multivorans, P. aeruginosa* , *P. lactis*, *A. baylyi*, *C. glutamicum,* and *Sphingobium* sp. (referred to as *Cn*H16_RS30120, *Bm*NP80_RS03580, *Pa*PA0247, *Pl*TX24_18430, *Ab*ACIAD1719, *Cg*CGTRNA_RS05390, and SpE2598_04620, respectively) were assembled, where *pobA*-like genes were placed under the control of the L-arabinose-inducible system AraC/P_{araBAD} (Supplementary Fig. S12). In the case of the constructs with the *pobA* gene, the addition of L-arabinose initiates the synthesis of PobA*,* which converts *p*-hydroxybenzoic acid into protocatechuic acid, RFP reporter gene expression was subsequently mediated by $PcaU^{AM}$ in the presence of protocatechuic acid. Since, to our knowledge, *E. coli* lacks the *pobA*-like gene, this bacterium transformed with constructs containing *Ab*P-caU^{AM}/P_{3B5} was employed for screening.

Fluorescence measurements were performed for constructs pEA034–41 and a single time-point was taken 6 h after the addition of either 5 mM *p*-hydroxybenzoic acid only (Fig. 6c) or 5 mM *p*-hydroxybenzoic acid and 1 mM L-arabinose (Supplementary Fig. S13). The screening results showed that 4-hydroxybenzoate 3-monooxygenase activity could not be differentiated when the culture medium was supplemented with 5 mM *p*-hydroxybenzoic acid and overexpression of *pobA*-like genes induced with 1 mM L-arabinose, the biosensor was fully saturated (Supplementary Fig. S13). However, in the absence of L-arabinose under uninduced AraC/P_{araBAD} state, the 4-hydroxybenzoate 3-monooxygenase activity could be differentiated with higher conversion of *p*-hydroxybenzoic acid into protocatechuic acid observed for PobA-like homologues from *Gammaproteobacteria* (*P. aeruginosa*, *P. lactis*, *A. baylyi*) and *Actinobacteria* (*C. glutamicum*) than that from *Betaproteobacteria* (*C. necator*, *B. multivorans)* and *Alphaproteobacteria* (*Sphingobium* sp.) under the same experimental conditions and host *E. coli* (Fig. 6c).

To further evaluate PobA activity results obtained using *Ab*$PcaU^{AM}$/P_{3B5}-based biosensor, *E. coli* cells harbouring the constructs pEA034–41 were grown overnight supplemented with 5 mM *p*-hydroxybenzoic acid. The supernatant samples were subjected to the quantification of extracellular *p*-hydroxybenzoic acid using HPLC, and protocatechuic acid using HPLC and *Cn*PcaQ/$P_{H16\_RS30145}$-based biosensor (Supplementary Fig. S14 and S15a,b). The concentrations of protocatechuic acid determined using the HPLC analysis showed a high accuracy and correlation ($r = 0.98$) of data obtained using the *Cn*PcaQ/$P_{H16\_RS30145}$-based biosensor (Supplementary Fig. S15c). Furthermore, the extracellular concentration of protocatechuic acid obtained with HPLC and the biosensor assay showed a correlation with intracellular PobA activity with a correlation coefficient r equal to 0.95 and 0.89, respectively (Supplementary Fig. S16a and b).

Discussion

The development and applications of analytical methods for the detection and measurement of phenolic acids have been multidimensional, from the study of these compounds for their biological roles as secondary metabolites to the evaluation of their health benefits. HPLC equipped with a photodiode array detector or liquid chromatography coupled with a mass spectrometer have been the most widespread analytical techniques used for the detection of phenolic acids extracellularly [3,47]. However, when it comes to intracellular studies and real-time monitoring of metabolites, these analytical approaches are slow and expensive to use, as they require the metabolite extraction and multiple sample processing is highly time consuming.

Recently, TF-based inducible gene expression systems have been used not only to control gene expression, but also to develop whole-cell biosensors suitable for monitoring the metabolite abundance intracellularly and extracellularly. Such biosensors have shown great potential as tools for the advancement of synthetic biology contributing to microbial cell factory development. In this study, we focus our effort on the identification of natural phenolic acids-specific inducible gene expression systems from different bacteria classes including *Alphaproteobacteria*, *Betaproteobacteria*, *Gammaproteobacteria*, *Actinobacteria*, and *Bacilli* and their characterisation using three bacterial chassis, namely, *E. coli*, *C. necator*, and *P. putida*. A pool of twenty-seven putative inducible systems (Table 1 and Supplementary Table S2) was identified through the literature and database searches, and they were subjected to further investigation for their ability to be activated by selected phenolic acids (Fig. 3a). Eighteen systems specific to eleven different phenolic acids were identified and further characterised.

Notably, the characterised inducible systems are controlled by six types of TFs including LysR, MarR, AraC/XylS, IclR, GntR, and PadR. Amongst these, only MarR, GntR, and PadR belonging to *Ct*MobR/P_{mobA}, *Pp*VanR/P_{vanA}, *Bm*PadR/$P_{BMD\_RS01890}$, *Bp*PadR/$P_{BPUM\_RS03685}$, *Pp*HcaR/$P_{PP\_RS17495}$, and *Ab*HcaR/$P_{ACIAD\_RS07960}$ were repressors, whereas remaining TFs acted as activators or dual-function-type regulators.

Developed TF-based biosensors exhibited different characteristics and responses to target phenolic acids in different genetic backgrounds. Intriguingly, the *Bm*PadR/$P_{BMD\_RS01890}$ and *Bp*PadR/$P_{BPUM\_RS03685}$ inducible systems mediated a significant increase in reporter gene expression in the presence of either *p*-coumaric or ferulic acid in *E. coli* (Fig. 3c and Supplementary Fig. S2 b). However, weak or no activation by *p*-coumaric and ferulic acid was observed with these systems in *C. necator* or *P. putida*, respectively (Fig. 3d,e and Supplementary Fig. S2c,d). This limited response could be explained by either of the following: (1) an absence or low availability of TF PadR, resulting from the poor expression (translation) of AT-rich genes from *B. megaterium* and *B. pumilus* in GC-rich bacteria due to a suboptimal codon usage [48], (2) a poor uptake of *p*-coumaric and ferulic acids by cells or (3) a rapid metabolism and conversion of these phenolic acids into metabolic intermediates that are unable to activate *Bm*PadR/$P_{BMD\_RS01890}$ and *Bp*PadR/$P_{BPUM\_RS03685}$.

To address the first option, the promoter only versions $P_{BMD\_RS01890}$ and $P_{BPUM\_RS03685}$ (Supplementary Figs. S4 and S5) were evaluated for gene expression. In all three bacterial chassis, these promoters exhibited 5- to 15-fold higher activity than that of corresponding inducible systems containing TF even in the absence of the inducer. This confirmed the previously reported role of PadR as a repressor of transcription [42] and ruled out the possibility that the expression of *padR* was impaired in *C. necator* or *P. putida*.

The poor uptake of *p*-coumaric and ferulic acids by cells as a cause of the absence of induction could also be excluded for *P. putida* KT2440, as hydroxycinnamic acids have been shown to be used as a carbon source [49] and therefore are taken up by this strain. In this study, a few other inducible systems, such as *Pp*HcaR/$P_{PP\_RS17495}$ and *Ab*HcaR/$P_{ACIAD\_RS07960}$, were shown to mediate a strong activation of reporter gene expression in *P. putida* when growth medium was supplemented with hydroxycinnamic acids (Fig. 5). Moreover, both *p*-coumaric acid and ferulic acid can be consumed by this bacterium, but not by *E. coli* or *C. necator* (Fig. 2). Therefore, it was possible that the induction in *C. necator* could be restricted by the limited uptake of *p*-coumaric and ferulic acids. Equally, the absence of catabolic activity toward *m*-coumaric acid or gentisic acid (Fig. 2) indicates that these phenolic acids are unlikely to be taken up by *C. necator* and *P. putida* or *E. coli* and *P. putida*, respectively.

With regard to hydroxycinnamic acid metabolism, it has been reported previously [49,50] that *p*-coumaric and ferulic acids were activated by conversion to *p*-coumaroyl-CoA and feruloyl-CoA by feruloyl-CoA synthetase (Fcs), which were then routed through the protocatechuate 4,5-cleavage pathway into the tricarboxylic acid (TCA) cycle for catabolic degradation. Moreover, Parke and Ornston [25] have shown that hydroxycinnamoyl-CoA thioesters, as inducers, relieve the repression of the hydroxycinnamate (*hca*) operon in *Acinetobacter baylyi* ADP1 by interacting with HcaR, the MarR-type transcriptional repressor. Therefore, *Pp*HcaR/$P_{PP\_RS17495}$ and *Ab*HcaR/$P_{ACIAD\_RS07960}$ inducible systems were activated exclusively in *P. putida* KT2440 cells and showed induction after 6 h due to the conversion of

hydroxycinnamates to hydroxycinnamoyl-CoA thioesters, potential inducers of HcaR-regulated systems. Although, the *hca* genes, exhibiting a relatively high homology to the *Acinetobacter* counterparts, have been identified in *C. necator* JMP134 [51], we were unable to find any relevant homologues in *C. necator* H16. Consistently, no activation of *Bm*PadR/$P_{BMD\_RS01890}$ and *Bp*PadR/$P_{BPUM\_RS03685}$ in *P. putida* was likely caused by the rapid conversion of hydroxycinnamic acids, their primary effector, to thioesters.

Phenolic acid-biosensors were subjected to thorough quantitative characterisation assessing induction level, dynamics and specificity in either *E. coli*, *C. necator*, or *P. putida* background. Three biosensors responding to *o*-hydroxybenzoic, *p*-hydroxybenzoic, and vanillic acid (*Cn*NahR/$P_{H16\_RS08125}$, *Cn*PobR/P_{pobA}, and *Cc*VanR^{AM}/P_{vanCC}, respectively), displayed low $^*K_m$ values with the gene expression tunable in the μM-range of phenolic acid concentration. First time to our knowledge, the specific *m*-hydroxybenzoic acid biosensor with a high induction level of 83.22-fold was developed.

Moreover, in this study, we successfully applied the protocatechuic acid-inducible biosensor for 4-hydroxybenzoate 3-monooxygenase (PobA) screening (Fig. 6). PobA proteins from *Gammaproteobacteria* and *Actinobacteria* (*P. aeruginosa*, *P. lactis*, *A. baylyi*, *C. glutamicum*) were identified to have higher conversion activity compared to PobA from *Alphaproteobacteria* and *Betaproteobacteria* (*Sphingobium* sp., *C. necator*, *B. multivorans*) under given conditions and in the same host.

To conclude, the multi-genome approach in this study enabled to build a comprehensive library of biosensors for detection of phenolic acids. They were thoroughly investigated generating rich quantitative data on their induction level, dynamics and specificity. Such systems can be applied for studying phenolic acid-metabolism, relevant enzyme identification, and screening. Moreover, they can assist in the metabolic engineering and synthetic biology applications.

CRediT authorship contribution statement

N.M. acquired funding. **N.M.** conceptualized the project. **N.M.** identified targets and designed tools. **E.A.**, **I.K.**, **E.V.**, **P.M.** and **N.M.** generated tools. **E.A.** and **N.M.** designed the experiments. **E.A.**, **I.K.**, **E.V.** and **I.J.** performed the experiments. **E.A.**, **I.K.** and **N.M.** analysed the results. **E.A.** and **N.M.** wrote the manuscript. All authors read and approved the final manuscript.

Declaration of Competing Interest

None declared.

Acknowledgements

This work was supported by the European Regional Development Fund (Project No. 01.2.2-LMT-K-718–02-0023)] under grant agreement with the Research Council of Lithuania (LMTLT) (to N.M.).

Appendix A. Supporting information

Supplementary data associated with this article can be found in the online version at doi:10.1016/j.nbt.2023.09.004.

References

[1] Russell W, Duthie G. Plant secondary metabolites and gut health: the case for phenolic acids. Proc Nutr Soc 2011;70:389–96. https://doi.org/10.1017/S0029665111000152.
[2] Huccetogullari D, Luo ZW, Lee SY. Metabolic engineering of microorganisms for production of aromatic compounds. Micro Cell Factor 2019;18:41. https://doi.org/10.1186/s12934-019-1090-4.
[3] Valanciene E, Jonuskiene I, Syrpas M, Augustiniene E, Matulis P, Simonavicius A, et al. Advances and prospects of phenolic acids production, biorefinery and analysis. Biomolecules 2020;10:874. https://doi.org/10.3390/biom10060874.
[4] Siedler S, Khatri NK, Zsohár A, Kjærbølling I, Vogt M, Hammar P, et al. Development of bacterial biosensor for rapid screening of yeast p-coumaric acid production. ACS Synth Biol 2017;6:1860–9. https://doi.org/10.1021/acssynbio.7b00009.
[5] Cheng F, Tang X-L, Kardashliev T. Transcription factor-based biosensors in high-throughput screening: advances and applications. Biotechnol J 2018;13:e1700648. https://doi.org/10.1002/biot.201700648.
[6] Wang Y, Li Q, Zheng P, Guo Y, Wang L, Zhang T, et al. Evolving the L-lysine high-producing strain of Escherichia coli using a newly developed high-throughput screening method. J Ind Microbiol 2016;43:1227–35. https://doi.org/10.1007/s10295-016-1803-1.
[7] Yang G, Withers SG. Ultrahigh-throughput FACS-based screening for directed enzyme evolution. Chembiochem 2009;10:2704–15. https://doi.org/10.1002/cbic.200900384.
[8] Machado LFM, Dixon N. Development and substrate specificity screening of an in vivo biosensor for the detection of biomass derived aromatic chemical building blocks. Commun Chem 2016;52:11402–5. https://doi.org/10.1039/C6CC04559F.
[9] Alvarez-Gonzalez G, Dixon N. Genetically encoded biosensors for lignocellulose valorization. Biotechnol Biofuels 2019;12:246. https://doi.org/10.1186/s13068-019-1585-6.
[10] Flachbart LK, Gertzen CGW, Gohlke H, Holger J, Marienhagen J. J. Development of a biosensor platform for phenolic compounds using a transition ligand strategy. ACS Synth Biol 2021;10:2002–14. https://doi.org/10.1021/acssynbio.1c00165.
[11] Flachbart LK, Sokolowsky S, Marienhagen J. Displaced by deceivers: prevention of biosensor cross-talk is pivotal for successful biosensor-based high-throughput screening campaigns. ACS Synth Biol 2019;8:1847–57. https://doi.org/10.1021/acssynbio.9b00149.
[12] Hanko EKR, Minton NP, Malys N. Design, cloning and characterization of transcription factor-based inducible gene expression systems. MethEnzymol 2019;621:153–69. https://doi.org/10.1016/bs.mie.2019.02.018.
[13] Kim NM, Sinnott RW, Sandoval NR. Transcription factor-based biosensors and inducible systems in non-model bacteria: current progress and future directions. Curr Opin Biotechnol 2020;64:39–46. https://doi.org/10.1016/j.copbio.2019.09.009.
[14] Mitchler MM, Garcia JM, Montero NE, Williams GJ. Transcription factor-based biosensors: a molecular-guided approach for natural product engineering. Curr Opin Biotechnol 2021;69:172–81. https://doi.org/10.1016/j.copbio.2021.01.008.
[15] Kaczmarek JA, Prather KLJ. Effective use of biosensors for high-throughput library screening for metabolite production. J Ind Microbiol 2021;48:kuab049. https://doi.org/10.1093/jimb/kuab049.
[16] Kanehisa M, Furumichi M, Tanabe M, Sato Y, Morishima K. KEGG: new perspectives on genomes, pathways, diseases and drugs. Nucleic Acids Res 2017;45:D353–61. https://doi.org/10.1093/nar/gkw1092.
[17] Jeske L, Placzek S, Schomburg I, Chang A, Schomburg D. BRENDA in 2019: a European ELIXIR core data resource. Nucleic Acids Res 2019;(D1):D542–9. https://doi.org/10.1093/nar/gky1048.
[18] Caspi R, Billington R, Fulcher CA, Keseler IM, Kothari A, Krummenacker M, et al. The MetaCyc database of metabolic pathways and enzymes. Nucleic Acids Res 2018;46:D633–9. https://doi.org/10.1093/nar/gkx935.
[19] Benson DA, Cavanaugh M, Clark K, Karsch-Mizrachi I, Lipman DJ, Ostell J, et al. GenBank. Nucleic Acids Res 2013;41:D36–42. https://doi.org/10.1093/nar/gks1195.
[20] Hanko EKR, Paiva AC, Jonczyk M, Abbott M, Minton NP, Malys N. A genome-wide approach for identification and characterisation of metabolite-inducible systems. Nat Commun 2020;11:1213. https://doi.org/10.1038/s41467-020-14941-6.
[21] Thanbichler M, Iniesta AA, Shapiro L. A comprehensive set of plasmids for vanillate - and xylose-inducible gene expression in Caulobacter crescentus. Nucleic Acids Res 2007;35:e137. https://doi.org/10.1093/nar/gkm818.
[22] Meyer AJ, Segall-Shapiro TH, Glassey E, Zhang J, Voigt CA. Escherichia coli "Marionette" strains with 12 highly optimized small-molecule sensors. Nat Chem Biol 2019;15:196–204. https://doi.org/10.1038/s41589-018-0168-3.
[23] Kunjapur AM, Prather KLJ. Development of a vanillate biosensor for the vanillin biosynthesis pathway in E. coli. ACS Synth Biol 2019;8:1958–67. https://doi.org/10.1021/acssynbio.9b00071.
[24] Gerischer U, Segura A, Ornston LN. PcaU, a transcriptional activator of genes for protocatechuate utilization in Acinetobacter. J Bacteriol 1998;180:1512–24. https://doi.org/10.1128/JB.180.6.1512-1524.1998.
[25] Parke D, Ornston N. Hydroxycinnamate (hca) catabolic genes from Acinetobacter sp. strain ADP1 are repressed by HcaR and are induced by hydroxycinnamoyl-coenzyme A thioesters. Appl Environ Microbiol 2003;69:5398–409. https://doi.org/10.1128/AEM.69.9.5398-5409.2003.
[26] DiMarco AA, Averhoff B, Ornston LN. Identification of the transcriptional activator pobR and characterization of its role in the expression of pobA, the structural gene for p-hydroxybenzoate hydroxylase in Acinetobacter calcoaceticus. J Bacteriol 1993;175:4499–506. https://doi.org/10.1128/jb.175.14.4499-4506.1993.
[27] Pérez-Pantoja D, Donoso R, Agulló L, Córdova M, Seeger M, Pieper DH, et al. Genomic analysis of the potential for aromatic compounds biodegradation in Burkholderiales. Environ Microbiol 2011;14:1091–117. https://doi.org/10.1111/j.1462-2920.2011.02613.x.
[28] Chen DW, Zhang Y, Jiang CY, Liu SJ. Benzoate metabolism intermediate benzoyl coenzyme a affects gentisate pathway regulation in Comamonas testosteroni. Appl Environ Microbiol 2014;80:4051–62. https://doi.org/10.1128/AEM.01146-14.
[29] Chao H, Zhou NY. GenR, an IclR-type regulator, activates and represses the transcription of gen genes involved in 3-hydroxybenzoate and gentisate catabolism in Corynebacterium glutamicum. J Bacteriol 2013;195:1598–609. https://doi.org/10.1128/JB.02216-12.

[30] Pacheco-Sánchez D, Molina-Fuentes Á, Marín P, Díaz-Romero A, Marqués S. DbdR, a new member of the LysR family of transcriptional regulators, coordinately controls four promoters in the Thauera aromatica AR-1 3,5-dihydroxybenzoate anaerobic degradation pathway. Appl Environ Microbiol 2019;85:e02295-18. https://doi.org/10.1128/AEM.02295-18.
[31] Kasai D, et al. γ-Resorcylate catabolic-pathway genes in the soil actinomycete Rhodococcus jostii RHA1. Appl Environ Microbiol 2015;81:7656–65. https://doi.org/10.1128/AEM.02422-15.
[32] Torres B, Porras G, Garcia JL, DiazE. Regulation of the mhp cluster responsible for 3-(3-hydroxyphenyl)propionic acid degradation in Escherichia coli. 27575-85 J Biol Chem 2003;278. https://doi.org/10.1074/jbc.M303245200.
[33] Hiromoto T, et al. Characterization of MobR, the 3-hydroxybenzoate-responsive transcriptional regulator for the 3-hydroxybenzoate hydroxylase gene of Comamonas testosteroni KH122–3 s. J Mol Biol 2006;364:863–77. https://doi.org/10.1016/j.jmb.2006.08.098.
[34] Quinn JA, McKay DB, Entsch B. Analysis of the pobA and pobR genes controlling expression of p-hydroxybenzoate hydroxylase in Azotobacter chroococcum. Gene 2001;264:77–85. https://doi.org/10.1016/S0378-1119(00)00599-0.
[35] Araki T, et al. The syringate o-demethylase gene of Sphingobium sp. strain SYK-6 is regulated by DesX, while other vanillate and syringate catabolism genes are regulated by DesR. Appl Environ Microbiol 2020;86. https://doi.org/10.1128/AEM.01712-20.
[36] Nogales J, Canales Á, Jiménez-Barbero J, Serra B, Pingarrón JM, García JL, et al. Unravelling the gallic acid degradation pathway in bacteria: the gal cluster from Pseudomonas putida. Mol Microbiol 2011;79:359–74. https://doi.org/10.1111/j.1365-2958.2010.07448.x.
[37] Arai H, et al. Genetic organization and characteristics of the 3-(3-hydroxyphenyl) propionic acid degradation pathway of Comamonas testosteroni TA441. J Microbiol 1999;145:2813–20. https://doi.org/10.1099/00221287-145-10-2813.
[38] Ngoc PT, et al. Phenolic acid-mediated regulation of the padC gene, encoding the phenolic acid decarboxylase of Bacillus subtilis. J Bacteriol 2008;190:3213–24. https://doi.org/10.1128/JB.01936-07.
[39] Calisti C, Ficca AG, Barghini P, Ruzzi M. Regulation of ferulic catabolic genes in Pseudomonas fluorescens BF13: Involvement of a MarR family regulator. Appl Microbiol Biotechnol 2008;80:475–83. https://doi.org/10.1007/s00253-008-1557-4.
[40] Providenti MA, O'Brien JM, Ruff J, Cook AM, Lambert IB. Metabolism of isovanillate, vanillate, and veratrate by Comamonas testosteroni strain BR6020. J Bacteriol 2006;188:3862–9. https://doi.org/10.1128/JB.01675-05.
[41] Hanko EKR, Minton NP, Malys N. Characterisation of a 3-hydroxypropionic acid-inducible system from Pseudomonas putida for orthogonal gene expression control in Escherichia coli and Cupriavidus necator. Sci Rep 2017;7:1724. https://doi.org/10.1038/s41598-017-01850-w.
[42] Gury J, Barthelmebs L, Tran NP, Diviès C, Cavin JF. Cloning, deletion, and characterization of PadR, the transcriptional repressor of the phenolic acid decarboxylase-encoding padA gene of Lactobacillus plantarum. Appl Environ Microbiol 2004;70:2146–53. https://doi.org/10.1128/AEM.70.4.2146-2153.2004.
[43] Notonier S, Werner AZ, Kuatsjah E, Dumalo L, Abraham PE, Hatmaker EA, et al. Metabolism of syringyl lignin-derived compounds in Pseudomonas putida enables convergent production of 2-pyrone-4,6-dicarboxylic acid. Metab Eng 2021;65:111–22. https://doi.org/10.1016/j.ymben.2021.02.005.
[44] Lazar JT, Shuvalova L, Rosas-Lemus M, Kiryukhina O, Satchell KJF, Minasov G. Structural comparison of p-hydroxybenzoate hydroxylase (PobA) from Pseudomonas putida with PobA from other Pseudomonas spp. and other monooxygenases. Acta Crystallogr F Struct Biol Commun 2019;75:507–14. https://doi.org/10.1107/S2053230X19008653.
[45] Westphal AH, Tischler D, Heinke F, Hofmann S, Gröning JAD, Labudde D, et al. Pyridine nucleotide coenzyme specificity of p-hydroxybenzoate hydroxylase and related flavoprotein monooxygenases. Front Microbiol 2018;9:3050. https://doi.org/10.3389/fmicb.2018.03050.
[46] Tamura K, Stecher G, Kumar S. MEGA11: molecular evolutionary genetics analysis version 11. Mol Biol Evol 2021;38:3022–7. https://doi.org/10.1093/molbev/msab120.
[47] Stalikas CD. Extraction, separation, and detection methods for phenolic acids and flavonoids. J Sep Sci 2007;30:3268–95. https://doi.org/10.1002/jssc.200700261.
[48] Hanson G, Coller J. Translation and protein quality control: Codon optimality, bias and usage in translation and mRNA decay. Nat Rev Mol Cell Biol 2018;19:20–30. https://doi.org/10.1038/nrm.2017.91.
[49] Jiménez JI, Miñambres B, García JL, Díaz E. Genomic analysis of the aromatic catabolic pathways from Pseudomonas putida KT2440. Environ Microbiol 2002;4:824–41. https://doi.org/10.1046/j.1462-2920.2002.00370.x.
[50] Graf N, Altenbuchner J. Genetic engineering of Pseudomonas putida KT2440 for rapid and high-yield production of vanillin from ferulic acid. Appl Microbiol Biotechnol 2014;98:137–49. https://doi.org/10.1007/s00253-013-5303-1.
[51] Pérez-Pantoja D, De La Iglesia R, Pieper DH, González B. Metabolic reconstruction of aromatic compounds degradation from the genome of the amazing pollutant-degrading bacterium Cupriavidus necator JMP134. FEMS Microbiol Rev 2008;32:736–94. https://doi.org/10.1111/j.1574-6976.2008.00122.x.